

# Silencing of FAM111B inhibits tumor growth and promotes apoptosis by decreasing AKT activity in ovarian cancer

Wei Wang<sup>1,2</sup>, Yun Gu<sup>2,3</sup>, Hao Ni<sup>1</sup>, Qiuying Quan<sup>1</sup> and Lingchuan Guo<sup>1</sup> 

<sup>1</sup>Department of Pathology, The First Affiliated Hospital of Soochow University, Suzhou 215006, China; <sup>2</sup>Department of Pathology, Women's Hospital of Nanjing Medical University (Nanjing Maternity and Child Health Care Hospital), Nanjing 210004, China;

<sup>3</sup>Department of Laboratory Medicine, The First Affiliated Hospital of Nanjing Medical University, Nanjing 210029, China  
Corresponding author: Lingchuan Guo. Email: szglc@hotmail.com

## Impact Statement

A huge body of evidence suggests that FAM111B (family with sequence similarity 111) plays a crucial role in several malignancies. Nonetheless, its role in ovarian cancer remains elusive. This study revealed that FAM111B was overexpressed in ovarian cancer tissues and various ovarian cancer cell lines, especially SKOV3 cells. By silencing FAM111B in SKOV3 cells, cellular proliferation, migration, and invasion were inhibited; in contrast, the cellular apoptotic rate was increased, and the cell cycle was arrested at the G1/S phase. In addition, western blot assays validated our finding that silencing of FAM111B decreased the protein levels of phospho-AKT (p-AKT) and promoted the protein expression of p53 and Caspase-1. The xenograft animal model demonstrated that FAM111B silencing inhibited tumor growth and the expression of Ki-67 and proliferating cell nuclear antigen (PCNA) while promoting cell apoptosis. As is well documented, AKT inactivation inhibits the progression of ovarian cancer. Therefore, we concluded that FAM111B plays an oncogenic role in ovarian cancer. FAM111B silencing is a potential therapeutic strategy against ovarian cancer.

## Abstract

Ovarian cancer is the most lethal gynecological tumor in women worldwide. FAM111B (family with sequence similarity 111 member B) is an oncoprotein associated with multiple cancers, but its biological functions in ovarian cancer remain elusive. In this study, FAM111B was overexpressed in ovarian cancer tissues and cell lines. Functional studies *in vitro* revealed that silencing of FAM111B inhibited ovarian cancer cell proliferation, invasion, and migration, as well as increased cell apoptosis. Furthermore, FAM111B silencing arrested the ovarian cancer cell cycle at the G1/S phase. Furthermore, western blot assays demonstrated that silencing of FAM111B resulted in downregulation of phospho-AKT (p-AKT) protein expression, as well as upregulation of p53 and caspase-1 protein expression. The xenograft animal model of ovarian cancer demonstrated that FAM111B silencing inhibited tumor growth, enhanced cell apoptosis, and inhibited Ki-67 and proliferating cell nuclear antigen (PCNA) protein expression *in vivo*. Conversely, the overexpression of FAM111B exhibited opposite effects on the ovarian cancer xenograft. It was previously established that inactivating AKT inhibited ovarian cancer progression. This study found that silencing of FAM111B inhibits tumor growth and promotes apoptosis by decreasing AKT activity in ovarian cancer. Caspase-1 and p53 signaling also influenced the function of FAM111B in SKOV3 cells. Collectively, our results demonstrate that silencing of FAM111B is a potential therapeutic strategy against ovarian cancer.

**Keywords:** FAM111B, ovarian cancer, p-AKT, tumor growth, apoptosis, p53

**Experimental Biology and Medicine 2023; 248: 1043–1055. DOI: 10.1177/15353702231160326**

## Introduction

Ovarian cancer is recognized as the most lethal gynecologic malignancy worldwide, which seriously threatens women's life and health.<sup>1</sup> According to statistical reports, more than 310,000 new cases of ovarian cancer and more than 207,000 deaths were expected in 2020 worldwide.<sup>2</sup> Despite advances in treatment modalities for ovarian cancer, including debulking surgery, chemotherapy, hormone therapy, immunotherapy, and targeted therapy,<sup>3</sup> almost 80% of patients with advanced-stage ovarian cancer relapse after treatment,

and the average 5-year survival rate is merely 49.1%.<sup>4,5</sup> Thus, investigating the molecular mechanisms associated with ovarian cancer is crucial for the development of effective therapeutic targets.

FAM111B (family with sequence similarity 111 member B) encodes a cysteine/serine peptidase protein similar to trypsin and is overexpressed in breast cancer<sup>6</sup> and lung adenocarcinoma.<sup>7,8</sup> Besides, mutations in FAM111B have been linked to inherited exocrine pancreatic dysfunction,<sup>9</sup> myopathy, and hereditary fibrosing poikiloderma with tendon contractures, and pulmonary fibrosis (POIKTMP).<sup>10–12</sup>

Furthermore, FAM111B levels rise early and decrease late during human adenovirus infection.<sup>13</sup> However, the mechanisms underlying FAM111B expression and function in ovarian cancer remain unknown.

Herein, FAM111B expressions were significantly upregulated in ovarian cancer tissues and various ovarian cancer cell lines. More importantly, knocking down FAM111B inhibited cell proliferation, reduced cell invasion and migration, and promoted cell apoptosis in SKOV3 cells. Additionally, western blot analysis revealed that FAM111B silencing downregulated the expression of phospho-AKT (p-AKT) and promoted the expression of p53 and caspase-1. Studies in nude mouse xenografts corroborated that silencing of FAM111B decreased cell growth and promoted apoptosis. Overall, FAM111B represents a potential therapeutic strategy against ovarian cancer.

## Materials and methods

### Patients and ethics approval

Human ovarian cancer specimens, adjacent healthy tissues 50 mm distant from the cancer lesions, and healthy ovaries were collected from patients who underwent surgery in Nanjing Maternity and Child Health Care Hospital. All participants signed the written informed consent form. The research protocol was approved by the Ethics Committee of Nanjing Maternity and Child Health Care Hospital (2019NFKSL-124).

### Bioinformatics analyses

FAM111B expression profiles in ovarian cancer were compiled from the TCGA (The Cancer Genome Atlas) and GEPIA (Gene Expression Profiling Interactive Analysis) databases (<http://gepia.cancer-pku.cn/detail.php?clicktag=degenes>). Based on the Kaplan–Meier plotter (<http://kmplot.com/analysis/index.php?p=service&cancer=ovar>), the overall survival (OS) rate of patients diagnosed with ovarian cancer was determined.

### Cell culture

RPMI-1640 (Gibco, USA) medium was supplemented with 10% fetal bovine serum (FBS), and 1% penicillin-streptomycin (100 IU/mL) was used to culture the human ovarian cancer cell lines HO8910, SKOV3, OVCAR3, and A2780 and the normal ovarian epithelial cells IOSE80 and HOSEpiC (ATCC, USA). Cells were cultured in a humidified atmosphere with 5% CO<sub>2</sub> at 37°C.

### Quantitative real-time polymerase chain reaction

TRIzol reagent purchased from ThermoFisher (USA) was used to extract total RNA. For quantitative real-time polymerase chain reaction (qPCR) analysis of FAM111B, HiScript III Reverse Transcriptase and SuperMix were procured from Vazyme (Nanjing, China). The expression of FAM111B was normalized to  $\beta$ -ACTIN as an endogenous control using the 2<sup>(- $\Delta\Delta C_t$ )</sup> method.<sup>14</sup> The primer sequences were the same as previously described.<sup>8</sup> Amplification reactions were conducted as follows: 94°C, 60 s; 94°C, 30 s; 60°C, 30 s; 72°C, 60 s; 40 cycles.

### Transfection of siRNAs

Transfection was achieved using 50 nM siRNA in all cases. The siRNA oligonucleotides were purchased from General Biology (Chuzhou, Anhui, China). The sequences were negative control (ctrl): 5'-UUCUCCGAACGUGUCACGUTT-3'; FAM111B siRNA: 5'-AGAAGAUUGUUAAGAUCAA-3'. After reaching 30–50% cell confluency, siRNAs mixed with 5  $\mu$ L of Lipofectamine 3000 (USA) were added to the culture medium as per the manufacturer's instructions. Proteins were extracted following siRNA transfection. Subsequently, cellular proliferation, apoptosis, cycle, migration, and invasion assays were conducted.

### Cell proliferation assay

The Cell Counting Kit-8 (CCK-8) kit (Vazyme, Nanjing, China) was used to analyze cell proliferation. Briefly, SKOV3 cells were transiently transfected with the negative ctrl or FAM111B siRNA. Twenty-four hours after transfection, the cells were digested, washed, counted, and plated into a 96-well plate (the density was 5000 cells per well) using five replicates per groups. After seeding in the 96-well plate for 0, 24, 48, and 72 h, 110  $\mu$ L of culture medium supplemented with 10  $\mu$ L of CCK-8 was transferred into each well. The absorbance was measured on a microplate reader (Molecular Devices, USA) after incubation for 1.5 h at 37°C.

### Cellular apoptosis assay

After siRNA transfection of SKOV3 cells for 12, 24, 36, and 48 h, the indicated negative ctrl or FAM111B siRNA groups were incubated with Annexin V-FITC/propidium iodide (PI) (Vazyme, Nanjing, China) to detect apoptosis following the manufacturer's protocol. Subsequently, flow cytometry (BD Biosciences, USA) was used to determine the level of cellular apoptosis.

### Cell cycle analysis

After siRNA transfection of SKOV3 cells for 12, 24, 36, and 48 h, the indicated negative ctrl or FAM111B siRNA groups were detected using a cell cycle kit (C6031, USEVERBRIGHT, China) following the manufacturer's instructions. Flow cytometry (BD Biosciences, USA) and the software Kaluza were then used to evaluate the cell cycle. Finally, the percentages of cells in different phases (G<sub>0</sub>/G<sub>1</sub>, S, and G<sub>2</sub>/M) were counted.

### Cell invasion assay

Transwell assay with Matrigel (Sigma, USA) was utilized to determine the invasiveness of ovarian cancer cells. After siRNA transfection of SKOV3 cells for 12, 24, 36, and 48 h, the indicated negative ctrl or FAM111B siRNA groups were incubated in a serum-free medium and then plated in Matrigel in the upper chamber of the Transwell apparatus (Corning Inc., New York, USA). In the bottom chambers, 10% FBS was added to the RPMI-1640 medium. After 48 h, the cells were incubated with 0.1% crystal violet. Finally, the invading cells were visualized under a microscope (Observer D1, Zeiss, Oberkochen, Germany). Migrated cells from four random fields were counted to determine cell invasiveness.

## Cell migration assay

Cell migration was evaluated using scratch wound-healing assays. After siRNA transfection for 12, 24, 36, and 48 h, the SKOV3 cells transfected with the indicated negative ctrl or FAM111B siRNA reached 100% confluency. Then, a scratch was made in each well using a pipette. The scratch was visualized under a microscope (Observer D1, Germany) at 0, 12, 24, 36, and 48 h.

## Murine xenograft assay

The empty vector pcDNA3.1- (abbreviated as pc-negative control [pc-NC]) and pcDNA3.1-FAM111B (pc-FAM111B) were purchased from Shanghai Sangon Biotech (China) and transiently transfected into SKOV3 cells using Lipofectamine 3000 (Invitrogen, CA, USA). The animal care committee at Nanjing Medical University (Nanjing, China) approved this study (IACUC-1911014). Sixteen 4- to 6-week-old female BALB/c nude mice (each weighing 15–20 g, each group comprising four mice, Nanjing Medical University, Nanjing, China) were used. The SKOV3 cells were transfected with the indicated pc-NC, pc-FAM111B, negative ctrl, or FAM111B siRNA and then subcutaneously injected into mice. Tumors were collected and weighed five weeks after the injection. Protein expression levels of FAM111B in subcutaneous tumors were detected. Formalin-fixed tumor tissues were sliced into paraffin-embedded sections for routine immunohistochemistry (IHC).

## Western blot analysis

Using Radio immunoprecipitation assay (RIPA) lysis buffer supplemented with 1 mM Phenylmethanesulfonyl fluoride (PMSF) (Beyotime, China), the proteins were isolated from the indicated cells or xenograft tumor tissues. Using sodium dodecyl sulfate-polyacrylamide gel electrophoresis, 15  $\mu$ g of total proteins were separated and then electrophoretically transferred to nitrocellulose membranes (Amersham, UK), and then immunoblotted with the primary antibodies. Next, chemiluminescence imaging (ECL, Amersham) was used to detect bound antibodies. A list of primary antibodies is presented in Table 1. Densitometry and Image J (National Institutes of Health, USA) were used to analyze band intensities in the western blots and normalize them to  $\beta$ -ACTIN.

## Immunohistochemistry

Formalin-fixed and paraffin-embedded ovarian cancer and adjacent tissues were then processed and sectioned, followed by IHC (Servicebio, Wuhan, China). An anti-FAM111B antibody (AP69852, Abcepta, Suzhou, China) was added to the paraffinized sections, followed by horseradish peroxidase (HRP)-labeled antibody, and finally treated with 3,3'-N-diaminobenzidine tetrahydrochloride (DAB). The nuclei were incubated with blue hematoxylin for histochemical staining. The expression of FAM111B was quantified according to the staining intensity scores (strong: 3; moderate: 2; weak: 1) and the proportion of positive cells (4, >75%; 3, 51–75%; 2, 25–50%; 1, <25%). The final IHC scores were determined by multiplying the intensity scores by the proportion of positive cells; the scores ranged from 1 to 12.

**Table 1.** Used primary and secondary antibodies in the western blot assay.

Name	Manufacture	Catalog number	Dilution
FAM111B	Bioss	bs-14694R	1/1000
p53	Proteintech	60283-2-Ig	1/1000
Bcl-2	Proteintech	12789-1-AP	1/1000
Bax	Proteintech	50599-2-Ig	1/1000
p-AKT	Proteintech	66444-1-Ig	1/1000
AKT	Proteintech	60203-2-Ig	1/1000
E-cadherin	Proteintech	20874-1-AP	1/1000
MMP-2	Proteintech	10373-2-AP	1/1000
MMP-9	Proteintech	10375-2-AP	1/1000
Cleaved Caspase 3	Abcam	ab32042	1/1000
Caspase 1	Proteintech	22915-1-AP	1/1000
$\beta$ -ACTIN	Proteintech	66009-1-Ig	1/3000
IL-1 $\beta$	Proteintech	16806-1-AP	1/1000
IL-18	Proteintech	10663-1-AP	1/1000
CCND1	Bioss	bsm-51692M	1/2000
CCND2	Proteintech	10934-1-AP	1/1000
CDK2	Proteintech	10122-1-AP	1/2000
CDK4	Bioss	bs-0633R	1/300
p-AKT	Proteintech	66444-1-Ig	1/1000
AKT	Proteintech	60203-2-Ig	1/1000
p21	Proteintech	10355-1-AP	1/2000
p27	Proteintech	25614-1-AP	1/2000
FAS	Proteintech	13098-1-AP	1/1000
FADD	Proteintech	14906-1-AP	1/1000
Caspase 8	Proteintech	13423-1-AP	1/500
DR3	Proteintech	55397-1-AP	1/1500
DR4	Proteintech	24063-1-AP	1/6000
Goat anti-mouse secondary antibody	Proteintech	SA00001-1	1/3000
Goat anti-rabbit secondary antibody	Proteintech	SA00001-2	1/3000

As outlined in Table 2, a final IHC score  $\geq 6$  indicated a high expression of FAM111B, whereas a final IHC score  $< 6$  was considered as a low expression of FAM111B.

Paraffin-embedded sections of subcutaneous tumors from xenograft mice were incubated with FAM111B (AP69852, Abcepta, Suzhou, China), p53 (60283-2-Ig, Proteintech, China), Ki-67 (27309-1-AP, Proteintech, China), and PCNA (10205-2-AP, Proteintech, China) antibodies. A microscope (Carl Zeiss, Oberkochen, Germany) was used to visualize and photograph the stained tissues. Ki-67-positive and PCNA-positive cells were analyzed by Image J (National Institutes of Health, USA). The H-score in the measurement area was calculated as follows: H-Score = (percentage of strong-intensity area  $\times 3$ ) + (percentage of moderate-intensity area  $\times 2$ ) + (percentage of weak-intensity area  $\times 1$ ).

## Terminal deoxynucleotidyl transferase-mediated nick-end labeling of UTP analysis

The DeadEnd™ TUNEL (terminal deoxynucleotidyl transferase-mediated nick-end labeling of UTP) System used to stain the paraffin-embedded xenograft tumor sections was purchased from Promega (USA). After staining the tissues, the coverslips were washed twice in phosphate-buffered saline (PBS). The 4,6-diamino-2-phenyl indole (DAPI, 1:2000) was used to blot the nuclei, and coverslips were then framed onto the glass slides with the Dako fluorescent mounting solution and visualized under a microscope (Carl Zeiss,

**Table 2.** Relationship between FAM111B expression and the clinical indicators of ovarian cancer patients.

Clinicopathologic features	Cases (n)	FAM111B expression		P value
		Low (n=36, %)	High (n=35, %)	
Age (years)				
<50	34	18 (52.94)	16 (47.06)	0.7178
≥50	37	18 (48.65)	19 (51.35)	$\chi^2=0.131$
FIGO staging				
Low stage (I–II)	44	27 (61.36)	17 (38.64)	0.0218*
High stage (III–IV)	27	9 (33.33)	18 (66.67)	$\chi^2=5.260$
T stage				
pT1	28	18 (64.29)	10 (35.71)	0.0632
pT2	16	9 (56.25)	7 (43.75)	$\chi^2=5.523$
pT3	27	9 (33.33)	18 (66.67)	
N stage				
pN0	58	32 (55.17)	26 (44.83)	0.1117
pN1	13	4 (30.77)	9 (69.23)	$\chi^2=2.530$
Histology				
Serous	36	13 (36.11)	23 (63.89)	0.0283*
Endometrioid	11	5 (45.45)	6 (54.55)	$\chi^2=9.079$
Clear cell	18	13 (72.22)	5 (27.78)	
Mucinous	6	5 (83.33)	1 (16.67)	
Differentiation				
High grade (G1)	18	14 (77.78)	4 (22.22)	0.0253*
Middle grade (G2)	29	13 (44.83)	16 (55.17)	$\chi^2=7.353$
Low grade (G3)	24	9 (37.50)	15 (62.50)	
Tumor size				
<8cm	31	12 (38.71)	19 (61.29)	0.0751
≥8cm	40	24 (60.00)	16 (40.00)	$\chi^2=3.167$
Metastasis				
Yes	38	13 (34.21)	25 (65.79)	0.0029*
No	33	23 (69.70)	10 (30.30)	$\chi^2=8.898$

\* $P < 0.05$  (chi-square test).

FIGO: The International Federation of Gynecology and Obstetrics.

Germany). Positive TUNEL ratio was calculated as: (All TUNEL-positive nuclei/All DAPI-positive nuclei)  $\times$  100%.

### Statistical analysis

GraphPad Prism 6.0 (San Diego, USA) was used for statistical analyses. Data were expressed as mean  $\pm$  standard deviation. In Table 2, clinical data were analyzed using the chi-square test, while in Figure 1(d), paired samples were analyzed using the *t*-test. For statistical comparison analysis, a two-tailed Student's *t*-test was utilized.  $P < 0.05$  was regarded as statistically significant.

## Results

### Expression and clinical significance of FAM111B in ovarian cancer

TCGA and GEPIA online databases were initially utilized to assess FAM111B expression in ovarian cancer. According to the data, FAM111B was significantly overexpressed in ovarian cancer tissues (Figure 1(a)). The online Kaplan–Meier plotter was used to determine the correlation between FAM111B expression and OS in ovarian cancer. A high level of FAM111B expression appeared to correlate with a lower OS rate in patients with ovarian cancer, although this difference was not significant (Figure 1(b)). Based on IHC

findings, the FAM111B protein expression was elevated in serous, endometrioid, and mucinous ovarian cancer tissues (Figure 1(c)). In ovarian cancer tissues, FAM111B was mainly located in the cytoplasm and nucleus (Figure 1(c)).

A total of 71 ovarian cancer samples were acquired for clinical analysis (Table 2). IHC staining was performed to determine the expression of FAM111B in ovarian cancer and adjacent tissues. Quantitative analysis revealed that the FAM111B expression was higher in ovarian cancer tissues than in adjacent tissues, as shown in Figure 1(d)). Besides, FAM111B was mostly expressed in serous ovarian cancer (Figure 1(c) and (d)). Table 2 presents the association between FAM111B expression and baseline demographics of patients with ovarian cancer. The results of chi-square test showed that FAM111B expression was significantly correlated with the International Federation of Gynecology and Obstetrics (FIGO) staging, histology subtype, differentiation grade, and metastasis. Thus, the high levels of expression of FAM111B were associated with advanced FIGO stage, serous epithelial ovarian cancer, poor differentiation, and metastasis (Table 2).

Next, the expression of FAM111B was determined via qPCR and western blot in various ovarian cancer cell lines HO8910, OVCAR3, SKOV3, and A2780 and the normal ovarian epithelial cells IOSE80 and HOSEpiC. Compared with normal ovarian epithelial cells, the ovarian cancer cell lines showed higher levels of FAM111B mRNA and protein



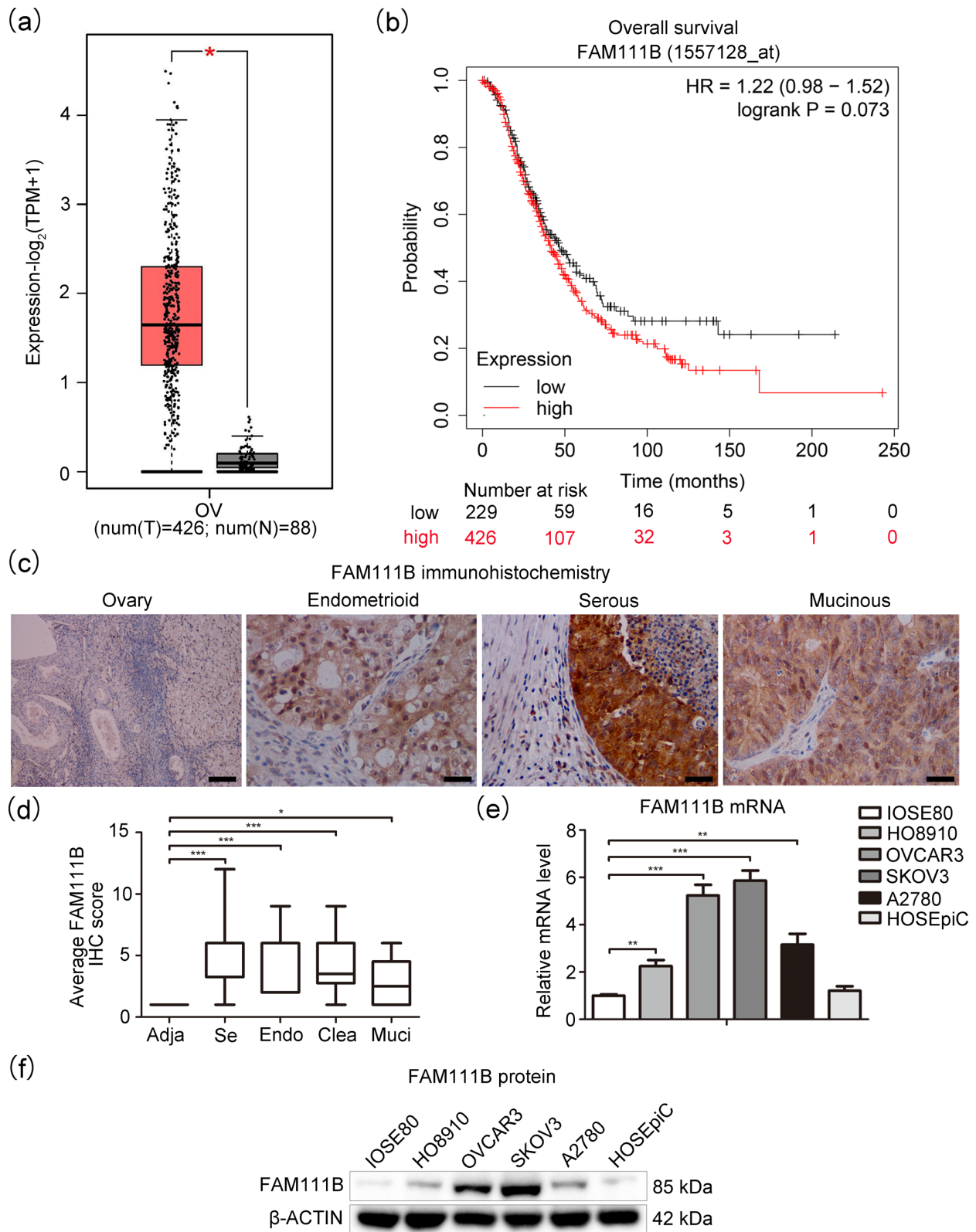


**Figure 1.** Analysis of FAM111B expression. (a) Expression of FAM111B in ovarian cancer, based on data retrieved from the TCGA and GEPIA databases that included 426 cases of TCGA ovarian serous cystadenocarcinoma and 88 cases of healthy ovary sequencing data. The bar indicates the median  $\pm$  quartile values. Student's unpaired *t*-test, \*\* $P < 0.01$ . (b) Relationship between FAM111B expression and overall survival in 655 ovarian cancer patients based on the online Kaplan-Meier plotter analysis. (c) Protein expression levels of FAM111B in ovarian cancer (scale bar=200  $\mu\text{m}$ ) and normal ovarian tissues (scale bar=50  $\mu\text{m}$ ) were determined via immunohistochemistry. (d) Expression of FAM111B protein in 71 ovarian cancer and adjacent tissues. The bar indicates the box and whiskers plus minimum to maximum values of the IHC score. Paired *t*-test compared with the adjacent tissues, \* $P < 0.05$ ; \*\*\* $P < 0.001$ . Analysis of FAM111B expression in normal ovarian epithelial cell lines (IOSE80 and HOSEpiC) and ovarian cancer cell lines (HO8910, OVCAR3, SKOV3, and A2780) using qPCR (e) and western blot assay (f). The bar indicates the mean  $\pm$  SD of three different experiments. Student's unpaired *t*-test compared with the IOSE80 group, \*\* $P < 0.01$ ; \*\*\* $P < 0.001$ .

expression (Figure 1(e) and (f)). Notably, the protein level of FAM111B was the highest in SKOV3 cells. Therefore, to assess the function of FAM111B in ovarian cancer cells, SKOV3 cells were selected for knockdown experiments.

### **Silencing FAM111B enhanced cell apoptosis and lowered cell proliferation and invasion**

The functions of FAM111B in ovarian cancer were assessed by knocking down FAM111B in SKOV3 cells using siRNAs. Western blot analysis showed that siRNA significantly decreased FAM111B levels in SKOV3 cells (Figure 2(a)). Furthermore, the CCK-8 assay revealed that silencing of FAM111B inhibited cell proliferation in SKOV3 cells (Figure 2(b)). The apoptotic level was determined by Annexin V-FITC/PI staining. When FAM111B was silenced in SKOV3 cells, the number of apoptotic cells was markedly elevated (Figure 2(c)). A flow cytometric analysis with PI staining was performed to detect alterations in the cell cycle. There was a significant elevation in the G0/G1 phase at 12, 24, 36, and 48 h in the FAM111B-silenced (FAM111B siRNA) group compared with the control. Compared with the G0/G1 phase in the negative ctrl, the G0/G1 phase in the FAM111B-silenced (FAM111B siRNA) group was significantly increased at 12, 24, 36, and 48 h, whereas a significant decrease in the S phase was seen at 24, 36, and 48 h, suggesting that cell cycle was arrested during the G1/S phase (Figure 2(d)).

Transwell invasion assay was used to assess cell invasiveness. Silencing of FAM111B significantly reduced the invasiveness of SKOV3 cells (Figure 3(a)). Cell migration was detected using the scratch test (Figure 3(b)). The results demonstrated that FAM111B silencing significantly decreased the migration of SKOV3 cells (Figure 3(b)). Thus, silencing of FAM111B reduced cell proliferation, invasion, and migration and induced apoptosis in SKOV3 cells.

### **Silencing of FAM111B inhibited ovarian cancer progression by promoting p53 and caspase-1 expression and repressing p-AKT expression**

Western blots were used to elucidate the molecular mechanisms of FAM111B function in ovarian cancer SKOV3 cells. These results showed that FAM111B silencing significantly promoted the expressions of cleaved caspase-3, Bax (apoptosis-related protein), and E-cadherin (migration-related protein), while inhibiting the expressions of Bcl-2 (anti-apoptotic protein B-cell lymphoma-2) and the invasion-related proteins MMP-2 and MMP-9 (Figure 4(a)). Earlier studies reported that downregulating p-AKT expression led to restricted cell proliferation and increased cell apoptosis in SKOV3 cells.<sup>15</sup> Additionally, p53 plays crucial roles in apoptosis, cell cycle arrest, autophagy, and metabolism.<sup>16</sup> The caspase-1 protein has been shown to induce apoptosis and play a decisive role in pathologic cell death.<sup>17</sup> A recent study demonstrated that ovarian tumors express higher levels of caspase-1, IL-1 $\beta$ , and IL-18 proteins than healthy ovaries.<sup>18</sup> The western blot demonstrated that p53 and caspase-1 protein expression levels were significantly elevated, whereas those of p-AKT were significantly decreased in the FAM111B knockdown group (Figure 4(a)).

Since FAM111B silencing induced downregulation of p-AKT and upregulation of p53, and arrested the cell cycle at

the G1/S phase, we then analyzed the expression of cell cycle arrest (G1/S) phase-related proteins, including cyclin D1 (CCND1), CCND2, cyclin-dependent kinases CDK2, CDK4, as well as their inhibitors p21 and p27. The results indicated that FAM111B silencing significantly inhibited the expression of CCND1, CCND2, CDK2, and CDK4 protein expression, whereas the expression of p21 and p27 was enhanced (Figure 4(b)).

Apoptosis can be divided into extrinsic and intrinsic types.<sup>19</sup> Since FAM111B silencing affected intrinsic apoptosis, and upregulated cleaved Caspase-3, we wondered whether the extrinsic apoptosis was altered. Therefore, we analyzed the expression levels of key extrinsic pathway-related proteins such as FAS, Fas-associated death domain (FADD), caspase-8, death receptor 3 (DR3), and death receptor 4 (DR4). The data showed that FADD, caspase-8, DR3, and DR4 were significantly upregulated in the FAM111B knockdown group (Figure 4(b)).

### **Silencing of FAM111B inhibited ovarian cancer growth *in vivo***

SKOV3 cells overexpressing FAM111B and pc-negative control cells (pc-NC) were subcutaneously injected into nude mice to analyze the role of FAM111B in ovarian cancer *in vivo*. Overexpression of FAM111B enhanced the growth of the subcutaneous xenograft, whereas silencing of FAM111B had an opposite effect (Figure 5(a)). Western blot and immunohistochemical staining assays demonstrated the overexpression and silencing efficiency of FAM111B (Figure 5(b) and (c)). Moreover, the p53, Ki-67, and PCNA immunohistochemical staining assays showed that FAM111B overexpression increased cell proliferation and decreased cellular apoptosis, whereas knockdown of FAM111B resulted in decreased proliferation and increased apoptosis (Figure 5(c)). The TUNEL assay revealed that FAM111B overexpression resulted in decreased cellular apoptosis, whereas silencing of FAM111B had the opposite effect (Figure 5(d)). Collectively, these results suggest that ovarian cancer cell proliferation and tumor growth were inhibited, and apoptosis was promoted *in vivo* by silencing FAM111B.

Western blot assay of the murine xenograft proteins showed that the levels of CCND1, CCND2, CDK2, and CDK4 were upregulated in the FAM111B overexpression group, whereas those of p21 and p27 were increased in the FAM111B knockdown group (Figure 6(a)). Furthermore, the levels of important extrinsic pathway-related proteins FAS, caspase-8, FADD, DR3, and DR4 were significantly decreased in the FAM111B overexpression group, but they were significantly increased in the FAM111B knockdown group (Figure 6(a)). Finally, the p-AKT level was significantly upregulated in the FAM111B overexpression group compared with the FAM111B knockdown group (Figure 6(a)).

### **Silencing of FAM111B promoted the expression of IL-1 $\beta$ and IL-18 in SKOV3 cells**

Given that silencing of FAM111B promoted caspase-1 expression (Figure 4(a)), the protein expression levels of

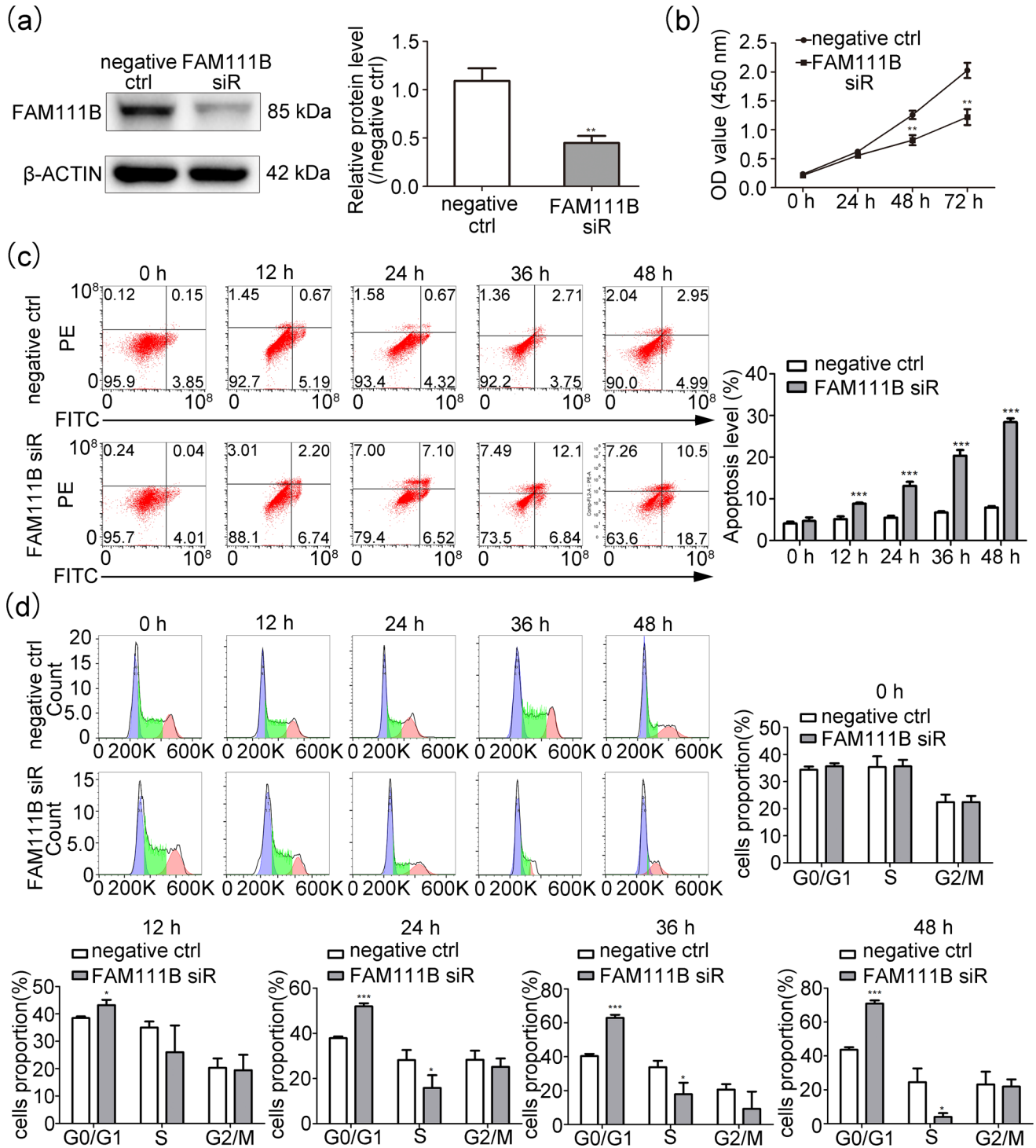


**Figure 2.** Silencing of FAM111B significantly reduced cell proliferation, arrested cell cycle, and promoted cell apoptosis. (a) Silencing efficiencies of FAM111B by siRNA transfection in SKOV3 cells, based on western blot analysis. The bar indicates the mean  $\pm$  SD of three different experiments. Students unpaired *t*-test,  $**P < 0.01$ . (b) Effects of FAM111B knockdown on the proliferation of SKOV3 cells, based on CCK-8 assay. Student's unpaired *t*-test,  $**P < 0.01$ . Effects of FAM111B knockdown on apoptosis (c) and cell cycle (d) of SKOV3 cells, based on flow cytometry. The bar indicates the mean  $\pm$  SD of three different experiments. Student's unpaired *t*-test,  $*P < 0.05$ ;  $**P < 0.01$ ;  $***P < 0.001$ . negative ctrl: negative control; FAM111B siR: FAM111B siRNA.

downstream effectors of caspase-1, including IL-1 $\beta$  and IL-18, were subsequently assessed. The results revealed that silencing of FAM111B upregulated the protein expression of IL-1 $\beta$  and IL-18 in SKOV3 cells (Figure 6(b)).

We speculate that FAM111B interacts with other proteins by encoding a protein with a peptidase domain similar to trypsin in the C-terminal. Next, the STRING database was used to predict the potential bound proteins of FAM111B.



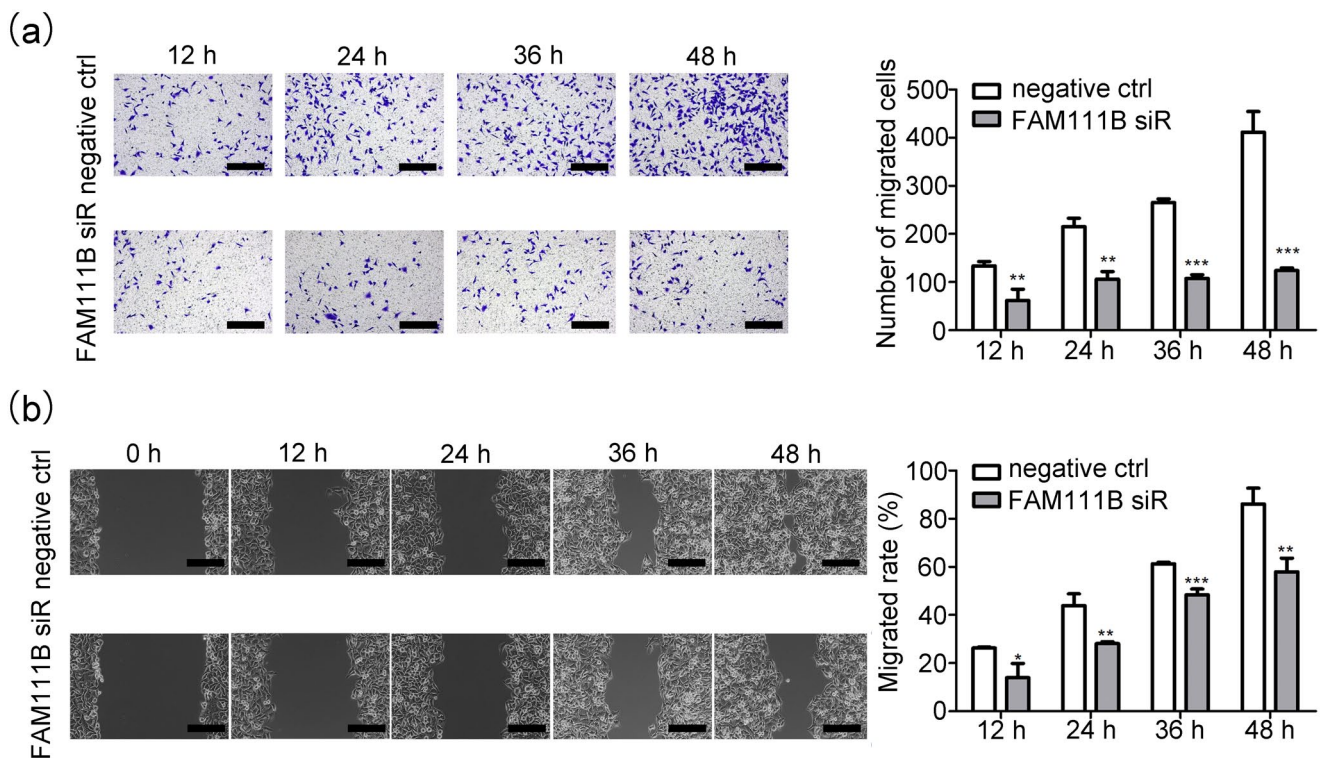


**Figure 3.** Silencing of FAM111B significantly inhibited migratory and invasive abilities. Effects of FAM111B knockdown on the invasiveness of SKOV3 cells, based on Transwell migration assay (a) and cell migration detected by scratch wound-healing assay (b). The bar indicates the mean  $\pm$  SD of three different experiments. Student's unpaired *t*-test, \* $P < 0.05$ ; \*\* $P < 0.01$ ; \*\*\* $P < 0.001$ . Scale bar = 200  $\mu$ m. negative ctrl: negative control; FAM111B siR: FAM111B siRNA.

The results indicated the known interactions of FAM111B with protein SET and predicted the interactions of FAM111B with C7orf57, MS4A15, and TEAD2 proteins (Figure 6(c)).

## Discussion

This study established that FAM111B was overexpressed in the ovarian cancer tissues as well as the ovarian cancer cell lines HO8910, OVCAR3, SKOV3, and A2780. Both *in vitro* functional and *in vivo* animal models revealed that silencing of FAM111B prevented ovarian cancer cell growth and promoted apoptosis. Thus, these findings imply that FAM111B plays an oncogenic role in ovarian cancer. Thus, it may be possible to treat ovarian cancer by inhibiting the expression of FAM111B.

Epithelial ovarian cancer accounts for 80–90% of ovarian cancer. The four subtypes of ovarian cancer include clear cell, mucinous carcinoma, endometrioid, and serous cancers.<sup>20</sup> IHC was used to determine the clinicopathologic significance of FAM111B in human ovarian cancer samples. Chi-square analysis confirmed that high expression levels of FAM111B were associated with the serous subtype of ovarian cancer, high-risk FIGO stage, and metastasis. Thus, FAM111B may be a potential prognostic marker of serous epithelial ovarian cancer, high-risk FIGO staging, and metastasis.

Prior studies reported higher levels of FAM111B expression in breast or lung cancer than in normal tissues.<sup>6–8</sup> Furthermore, a knockdown of FAM111B prevented breast or lung cancer cell proliferation, migration, and invasion. Consistent with these results, our data revealed that

silencing of FAM111B prevented cell proliferation, migration, and invasion; increased the apoptotic rate; and arrested the cell cycle at G1/S phase in ovarian cancer SKOV3 cells. These results suggest that FAM111B plays an oncogenic role in various malignancies. Thus, decreased cell migration or invasion may be attributed to reduced cell viability in the FAM111B knocking down group. A recent study demonstrated the regulatory role of FAM111B in migration and invasion.<sup>21</sup> Thus, FAM111B may play a role in migration and invasion of ovarian cancer cells.

It was reported that the FAM111B protein modulates p16 levels in lung adenocarcinomas via p16 degradation, thereby regulating cell cycle progression.<sup>7</sup> Moreover, FAM111B was found to be a direct target of p53 and was related to growth, G1/S arrest, and apoptosis.<sup>8</sup> Herein, silencing of FAM111B upregulated p53 protein expression while decreasing that of p-AKT. p53 is known to be a tumor suppressor and a master regulator of cell cycle arrest, apoptosis, autophagy, and metabolism.<sup>16</sup> Therefore, silencing of FAM111B may arrest the cell cycle by promoting p53 protein expression. Activation of p53 induces the transcription of CDK inhibitor p21, inhibiting cyclin E-CDK2 complexes and causing G1 arrest.<sup>22</sup>

AKT, also referred to as protein kinase, is a canonical downstream effector of PI3K.<sup>23</sup> Activated Akt modulates cell cycle progression, survival, apoptosis, and growth.<sup>24</sup> Inactivating the PI3K/AKT signaling pathway led to inhibition of ovarian cancer progression.<sup>25</sup> Interestingly, the inhibition of miR-21 decreased the expression of p-AKT, restricted proliferation, and promoted apoptosis in SKOV3 cells.<sup>15</sup>



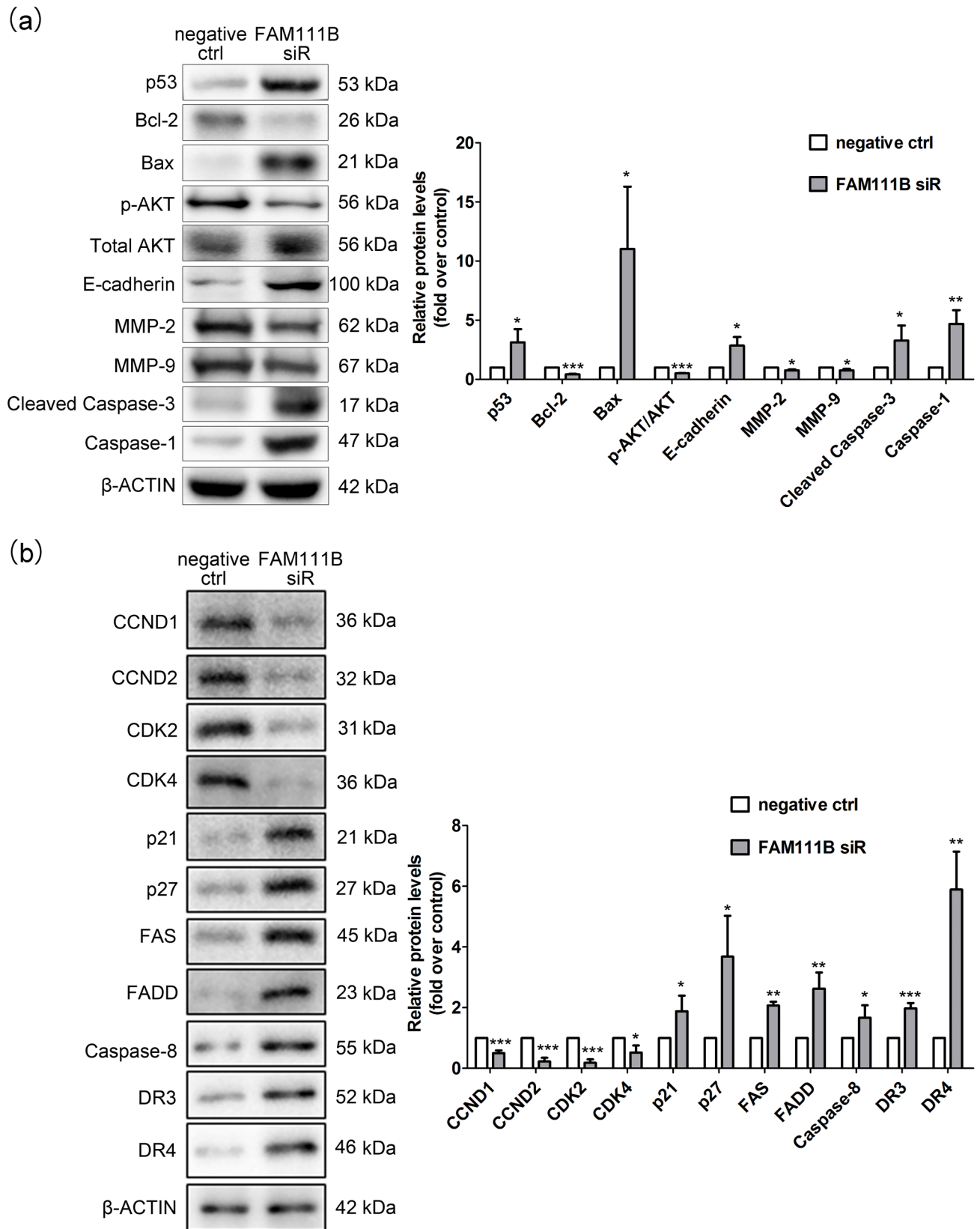


**Figure 4.** Silencing of FAM111B promoted protein expression of p53 and caspase-1 and inhibited p-AKT protein expression. (a) Effects of FAM111B knockdown on the expression of apoptosis-, migration-, and invasion-related proteins were determined via western blot analysis. (b) Effects of FAM111B knockdown on the protein expression of cell cycle- and apoptosis-related proteins, based on western blot analysis. The bar indicates the mean  $\pm$  SD of two or three different experiments. Student's unpaired *t*-test, \*\* $P < 0.01$ ; \*\*\* $P < 0.001$ . The intensity of each protein was normalized to  $\beta$ -ACTIN. Specifically, the protein expression of p-AKT was normalized to that of total AKT. negative ctrl: negative control; FAM111B siR: FAM111B siRNA.

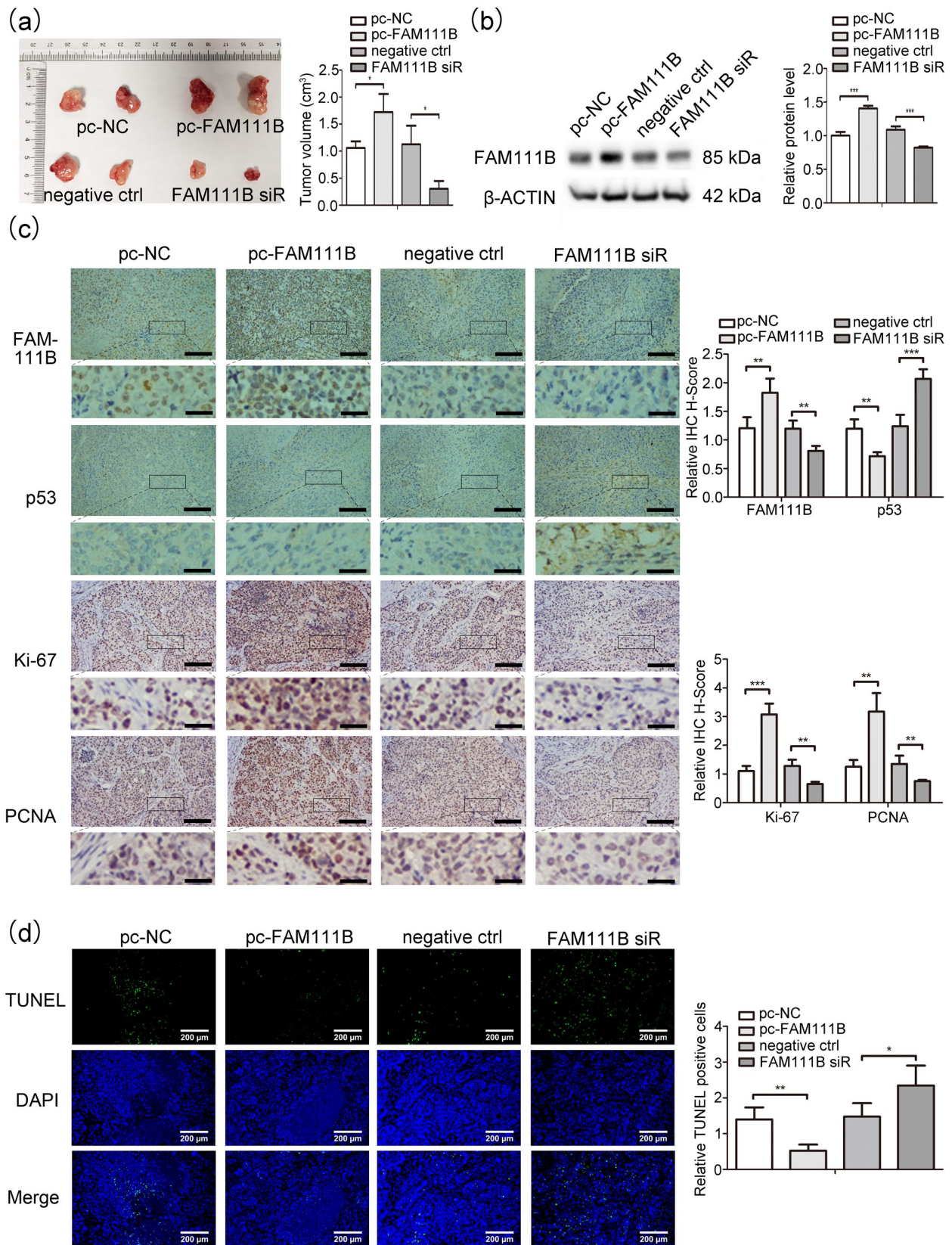


**Figure 5.** Silencing of FAM111B inhibited tumor growth and promoted apoptosis *in vivo*. (a) Excised tumors of the mice injected with the indicated cells at five weeks are illustrated on the left. The average weight of the indicated mice ( $n=4$ ) is depicted on the right. The bar indicates the mean  $\pm$  SD of three different experiments. Student's unpaired *t*-test, \* $P < 0.05$ . (b) Efficiencies of FAM111B overexpression or knockdown determined by western blot assay. Student's unpaired *t*-test, \*\*\* $P < 0.001$ . (c) Effects of overexpression or silencing of FAM111B on the protein expression of FAM111B and p53 as well as cell proliferation-related proteins Ki-67 and PCNA based on immunohistochemical analysis. Scale bar = 100  $\mu$ m. Magnification scale bar = 25  $\mu$ m. (d) Effects of overexpression or silencing of FAM111B on cellular apoptosis determined by TUNEL assay. Every bar indicates the mean  $\pm$  SD of two different experiments. Student's unpaired *t*-test, \* $P < 0.05$ . \*\* $P < 0.01$ . Scale bar = 200  $\mu$ m. IHC: immunohistochemistry; Ki-67: proliferation marker protein Ki-67; PCNA: proliferating cell nuclear antigen; TUNEL: transferase dUTP nick-end labeling; pc-NC: pcDNA3.1-control; pc-FAM111B: FAM111B overexpression; negative ctrl: negative control; FAM111B siR: FAM111B siRNA.

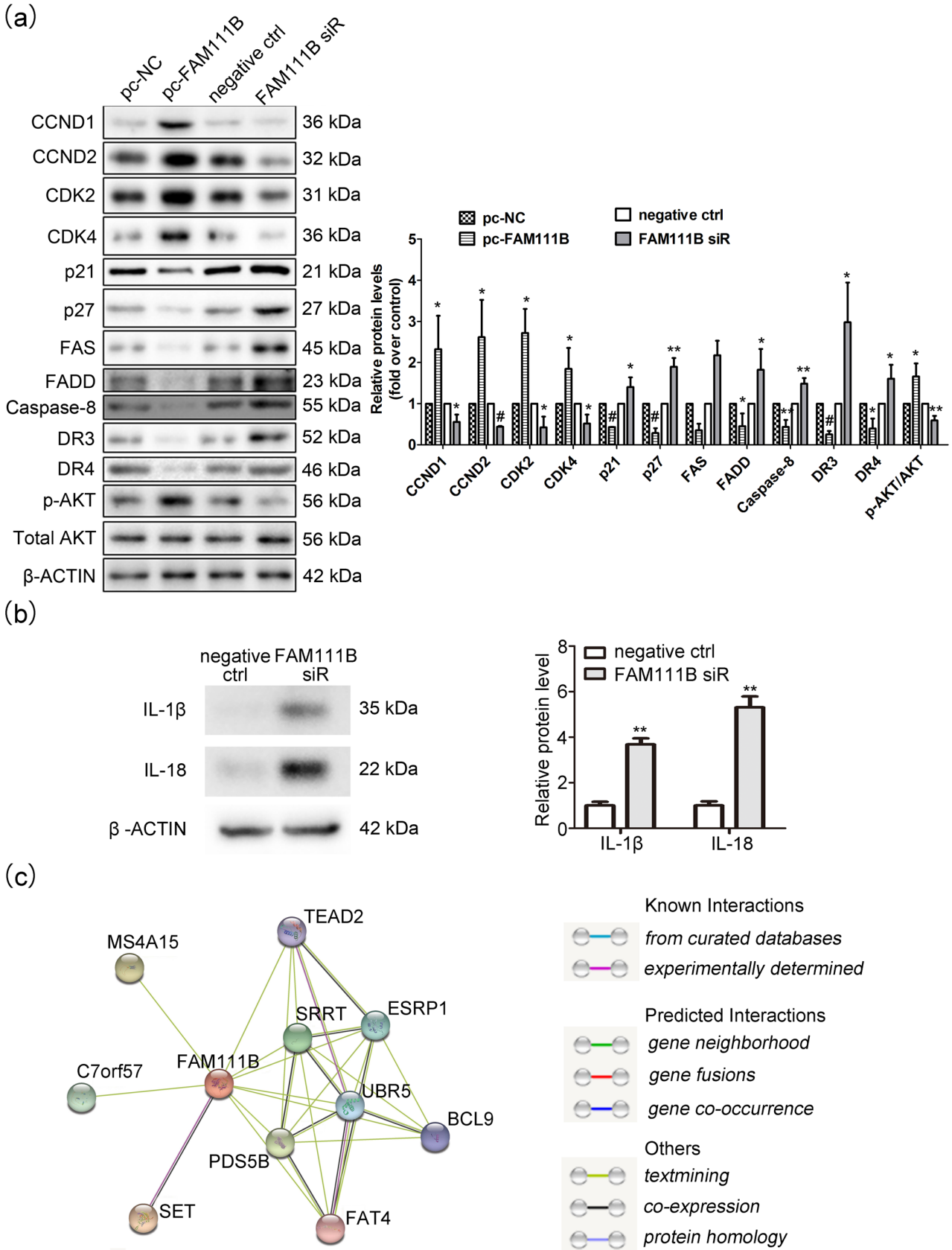


**Figure 6.** Effects of FAM111B on the expression of cell cycle- and apoptosis-related proteins *in vivo*, and STRING analysis. (a) Effects of overexpression or silencing of FAM111B on the protein expression of cell cycle- and apoptosis-related proteins as well as p-AKT in the murine xenograft model based on western blot analysis. \* $P < 0.05$ ; \*\* $P < 0.01$ ; \*\*\* $P < 0.001$ . Mark-up of the pc-FAM111B indicates comparison between the pc-NC and pc-FAM111B; mark-up of the FAM111B siR suggests comparison between negative ctrl and FAM111B siR. (b) Effects of FAM111B knockdown on the protein expression of IL- $\beta$  and IL-18 in SKOV3 cells based on western blot analysis. The bar indicates the mean  $\pm$  SD of two or three different experiments. Student's unpaired *t*-test, \*\* $P < 0.01$ ; \*\*\* $P < 0.001$ . negative ctrl: negative control; FAM111B siR: FAM111B siRNA. (c) STRING (<https://cn.string-db.org/network/9606.ENSP00000341565>) analysis of the protein-protein interaction network of FAM111B.



In line with these studies, our study found that silencing of FAM111B led to inhibition of p-AKT expression, indicating that FAM111B silencing suppressed cell proliferation, enhanced the apoptotic rate, and arrested the cell cycle by downregulating p-AKT expression.

P53 function may be regulated via Akt-mediated Mdm2 expression.<sup>26</sup> Elevated MDM2 inhibits P53 transcriptional activity by promoting its degradation, resulting in cancer progression.<sup>27</sup> p-AKT was reported to promote proliferation via the MDM2/P53 pathway and inhibit apoptosis via the BCL-2/BAX/Cytochrome-C/Caspase-3/Caspase-9 pathway; it promoted invasion and migration via Snail/E-cadherin/N-cadherin/Vimentin pathway.<sup>27</sup>

Oncogenic AKT induces the transcription of CCND1, CCND2, and CDK4 to regulate G1-S cell cycle transition.<sup>22</sup> P27 is repressed by AKT and enhanced by p53 during the regulation of G1-S cell cycle transition.<sup>22</sup> These studies support our results that decreased AKT activity and increased p53 protein expression by silencing FAM111B lead to reduced expression of CCND1, CCND2, CDK2, and CDK4 and increased expression of p21 and p27.

Molecular mechanisms regulating apoptosis and non-apoptotic types of regulated cell death have been extensively analyzed.<sup>28</sup> Extrinsic apoptosis is mediated by membrane receptors and death receptors, and triggered by initiator caspase CASP8 (caspase-8). Conversely, intrinsic apoptosis is triggered by mitochondrial outer membrane permeabilization (MOMP). Several members of the BCL2 family are involved in regulating MOMP, including pro-apoptotic (BAX) and anti-apoptotic members (BCL2). Using an intronic p53 binding site, p53 upregulates death receptor 4.<sup>29</sup> P53 was found to affect both extrinsic and intrinsic apoptosis,<sup>19</sup> therefore silencing FAM111B may affect both extrinsic and intrinsic apoptosis via upregulation of p53.

Caspase-1 belongs to the cysteine-aspartic acid protease (caspase) family and stimulates the synthesis of IL-1 $\beta$  and IL-18, which participate in the inflammatory processes,<sup>17</sup> resulting in lytic cell death, known as pyroptosis.<sup>30</sup> Caspase-1 protein has been reported to induce apoptosis and is implicated in pathologic cell death.<sup>17</sup> The current study revealed that the levels of caspase-1, IL-18, and IL-1 $\beta$  protein expression were higher in ovarian tumors than in normal ovaries.<sup>18</sup> Our work further indicated that silencing of FAM111B upregulated the protein expression of caspase-1, IL-18, and IL-1 $\beta$ . These results suggest that silencing of FAM111B promotes cellular apoptosis by upregulating caspase-1 protein expression in SKOV3 cells. Furthermore, p53 was reported to promote caspase-1 expression and enhance the expression of IL-1 $\beta$  and IL-18, to induce pyroptosis.<sup>31</sup> Upregulation of p53 in the FAM111B knockdown group may lead to increased levels of caspase-1, followed by IL-1 $\beta$  and IL-18. However, further studies are warranted to determine whether pyroptosis is related to the function of FAM111B in ovarian cancer.

Bioinformatics analysis revealed that FAM111B interacts with several proteins, including SET, FAT4, and PDS5B. SET is involved in several intracellular events, including apoptosis, transcription, nucleosome assembly, and histone chaperoning. However, further pull-down assays and co-immunoprecipitation are necessary to explore the detailed molecular mechanisms of FAM111B.

Taken together, our results reveal that ovarian cancers exhibit high levels of FAM111B expression. Furthermore, silencing of FAM111B inhibited the progression of ovarian cancer by inhibiting p-AKT and increasing p53 expression. Silencing of FAM111B inhibited cell proliferation via p-AKT/P53 pathway, promoted apoptosis via p-AKT/BCL2/BAX/Caspase-3 or p53/FADD/Caspase-8 pathway, and reduced migration and invasion via p-AKT/E-cadherin and MMP2/MMP9 pathways. Therefore, silencing of FAM111B is a potential therapeutic approach against ovarian cancer.

#### AUTHORS' CONTRIBUTIONS

All the authors participated in the design, implementation, and analysis of the experiments. Study conception, results analysis, and article drafting was performed by WW, YG, and HN, while QQ conducted the experiments and performed the bioinformatics and statistical analyses. In addition to editing the article, LG designed the experiment and guided the students.

#### DECLARATION OF CONFLICTING INTERESTS

The author(s) declared no potential conflicts of interest with respect to the research, authorship, and/or publication of this article.

#### ETHICAL APPROVAL

Human ovarian cancer specimens, adjacent normal tissues 50 mm away from the cancer lesions, and normal ovaries were collected from patients who underwent surgery in Nanjing Maternity and Child Health Care Hospital. All participants were requested to sign the written informed consent form. The research protocol was approved by the Ethics Committee of Nanjing Maternity and Child Health Care Hospital (2019NFKSL-124).

#### FUNDING

The author(s) disclosed receipt of the following financial support for the research, authorship, and/or publication of this article: This work was supported by the National Natural Science Foundation of China (81802105) and the Jiangsu Provincial Key Research and Development Program (Grant No. BE2017619).

#### DATA AVAILABILITY

Upon reasonable request, the data that support the findings of this study are available from the corresponding author.

#### ORCID ID

Lingchuan Guo  <https://orcid.org/0000-0002-1028-9296>

#### SUPPLEMENTAL MATERIAL

Supplemental material for this article is available online.

#### REFERENCES

1. Siegel RL, Miller KD, Fuchs HE, Jemal A. Cancer statistics, 2022. *CA Cancer J Clin* 2022;72:7–33
2. Sung H, Ferlay J, Siegel RL, Laversanne M, Soerjomataram I, Jemal A, Bray F. Global cancer statistics 2020: GLOBOCAN estimates of incidence and mortality worldwide for 36 cancers in 185 countries. *CA Cancer J Clin* 2021;71:209–49
3. Kuroki L, Guntupalli SR. Treatment of epithelial ovarian cancer. *BMJ* 2020;371:m3773

4. Salani R, Khanna N, Frimer M, Bristow RE, Chen LM. An update on post-treatment surveillance and diagnosis of recurrence in women with gynecologic malignancies: Society of Gynecologic Oncology (SGO) recommendations. *Gynecol Oncol* 2017;**146**:3–10
5. Howlander N, Noone AM, Krapcho M, Miller D, Brest A, Yu M, Ruhl J, Tatalovich Z, Mariotto A, Lewis DR, Chen HS, Feuer EJ, Cronin KA (eds). *SEER Cancer Statistics Review, 1975-2018*. Bethesda, MD: National Cancer Institute, 2020. [https://seer.cancer.gov/csr/1975\\_2018/](https://seer.cancer.gov/csr/1975_2018/)
6. Li W, Hu S, Han Z, Jiang X. YY1-Induced transcriptional activation of FAM111B contributes to the malignancy of breast cancer. *Clin Breast Cancer* 2022;**22**:e417–25
7. Kawasaki K, Nojima S, Hijiki S, Tahara S, Ohshima K, Matsui T, Hori Y, Kurashige M, Umeda D, Kiyokawa H, Kido K, Okuzaki D, Morii E. FAM111B enhances proliferation of KRAS-driven lung adenocarcinoma by degrading p16. *Cancer Sci* 2020;**111**:2635–46
8. Sun H, Liu K, Huang J, Sun Q, Shao C, Luo J, Xu L, Shen Y, Ren B. FAM111B, a direct target of p53, promotes the malignant process of lung adenocarcinoma. *Onco Targets Ther* 2019;**12**:2829–42
9. Seo A, Walsh T, Lee MK, Ho PA, Hsu EK, Sidbury R, King MC, Shimamura A. FAM111B mutation is associated with inherited exocrine pancreatic dysfunction. *Pancreas* 2016;**45**:858–62
10. Arowolo A, Rhoda C, Khumalo N. Mutations within the putative protease domain of the human FAM111B gene may predict disease severity and poor prognosis: a review of POIKTMP cases. *Exp Dermatol* 2022;**31**:648–54
11. Zhang Z, Zhang J, Chen F, Zheng L, Li H, Liu M, Li M, Yao Z. Family of hereditary fibrosing poikiloderma with tendon contractures, myopathy and pulmonary fibrosis caused by a novel FAM111B mutation. *J Dermatol* 2019;**46**:1014–8
12. Mercier S, Kury S, Shaboodien G, Houniet DT, Khumalo NP, Bou-Hanna C, Bodak N, Cormier-Daire V, David A, Faivre L, Figarella-Branger D, Gherardi RK, Glen E, Hamel A, Laboisse C, Le Caignec C, Lindenbaum P, Magot A, Munnich A, Mussini JM, Pillay K, Rahman T, Redon R, Salort-Campana E, Santibanez-Koref M, Thauvin C, Barbarot S, Keavney B, Bezieau S, Mayosi BM. Mutations in FAM111B cause hereditary fibrosing poikiloderma with tendon contracture, myopathy, and pulmonary fibrosis. *Am J Hum Genet* 2013;**93**:1100–7
13. Ip WH, Wilkens B, Solomatina A, Martin J, Melling M, Hidalgo P, Bertzbach LD, Speiseder T, Dobner T. Differential regulation of cellular FAM111B by human adenovirus C type 5 E1 oncogenes. *Viruses* 2021;**13**:1015
14. Livak KJ, Schmittgen TD. Analysis of relative gene expression data using real-time quantitative PCR and the 2(-Delta Delta C(T)) method. *Methods* 2001;**25**:402–8
15. Liu HY, Zhang YY, Zhu BL, Feng FZ, Yan H, Zhang HY, Zhou B. miR-21 regulates the proliferation and apoptosis of ovarian cancer cells through PTEN/PI3K/AKT. *Eur Rev Med Pharmacol Sci* 2019;**23**:4149–55
16. Farnebo M, Bykov VJ, Wiman KG. The p53 tumor suppressor: a master regulator of diverse cellular processes and therapeutic target in cancer. *Biochem Biophys Res Commun* 2010;**396**:85–9
17. Feng Q, Li P, Salamanca C, Huntsman D, Leung PC, Auersperg N. Caspase-1 alpha is down-regulated in human ovarian cancer cells and the overexpression of caspase-1alpha induces apoptosis. *Cancer Res* 2005;**65**:8591–6
18. Luborsky J, Barua A, Edassery S, Bahr JM, Edassery SL. Inflammasome expression is higher in ovarian tumors than in normal ovary. *PLoS ONE* 2020;**15**:e0227081
19. Carneiro BA, El-Deiry WS. Targeting apoptosis in cancer therapy. *Nat Rev Clin Oncol* 2020;**17**:395–417
20. Ramalingam P. Morphologic, immunophenotypic, and molecular features of epithelial ovarian cancer. *Oncology* 2016;**30**:166–76
21. Zhu X, Xue C, Kang X, Jia X, Wang L, Younis MH, Liu D, Huo N, Han Y, Chen Z, Fu J, Zhou C, Yao X, Du Y, Cai W, Kang L, Lyu Z. DNMT3B-mediated FAM111B methylation promotes papillary thyroid tumor glycolysis, growth and metastasis. *Int J Biol Sci* 2022;**18**:4372–87
22. Otto T, Sicinski P. Cell cycle proteins as promising targets in cancer therapy. *Nat Rev Cancer* 2017;**17**:93–115
23. Fresno VJ, Casado E, de Castro J, Cejas P, Belda-Iniesta C, Gonzalez-Baron M. PI3K/Akt signalling pathway and cancer. *Cancer Treat Rev* 2004;**30**:193–204
24. Franke TF, Hornik CP, Segev L, Shostak GA, Sugimoto C. PI3K/Akt and apoptosis: size matters. *Oncogene* 2003;**22**:8983–98
25. Yalan S, Yanfang L, He C, Yujie T. Circular RNA circRHOBTB3 inhibits ovarian cancer progression through PI3K/AKT signaling pathway. *Panminerva Med* 2020. Epub ahead of print 27 July 2020. DOI:10.23736/S0031-0808.20.03957-9
26. Takahashi K, Miyashita M, Makino H, Akagi I, Orita H, Hagiwara N, Nomura T, Gabrielson EW, Tajiri T. Expression of Akt and Mdm2 in human esophageal squamous cell carcinoma. *Exp Mol Pathol* 2009;**87**:42–7
27. Ayesha M, Majid A, Zhao D, Greenaway FT, Yan N, Liu Q, Liu S, Sun MZ. MiR-4521 plays a tumor repressive role in growth and metastasis of hepatocarcinoma cells by suppressing phosphorylation of FAK/AKT pathway via targeting FAM129A. *J Adv Res* 2022;**36**:147–61
28. Tang D, Kang R, Berghe TV, Vandenabeele P, Kroemer G. The molecular machinery of regulated cell death. *Cell Res* 2019;**29**:347–64
29. Liu X, Yue P, Khuri FR, Sun SY. p53 upregulates death receptor 4 expression through an intronic p53 binding site. *Cancer Res* 2004;**64**:5078–83
30. Bergsbaken T, Fink SL, Cookson BT. Pyroptosis: host cell death and inflammation. *Nat Rev Microbiol* 2009;**7**:99–109
31. Su Y, Sai Y, Zhou L, Liu Z, Du P, Wu J, Zhang J. Current insights into the regulation of programmed cell death by TP53 mutation in cancer. *Front Oncol* 2022;**12**:1023427

(Received April 21, 2022, Accepted February 9, 2023)